recycling

MDPI

*Article*

# New Strategy for Upcycling Marine Plastic Waste Through the Development of a Diamine-Functionalized Poly(ethylene terephthalate) Compatibilizer

**Pedro V. Rodrigues, Sibele P. Cestari, Vasco Cruz, M. Cidália R. Castro * and Ana Vera Machado**

Department of Polymer Engineering, Institute for Polymers and Composites (IPC), Campus de Azurém, University of Minho, 4804-533 Guimarães, Portugal; pedro.rodrigues@dep.uminho.pt (P.V.R.); sibele.cestari@piep.pt (S.P.C.); vasco.cruz@dep.uminho.pt (V.C.); avm@dep.uminho.pt (A.V.M.)
* Correspondence: cidaliacastro@dep.uminho.pt; Tel.: +351-253510320

**Abstract:** A compatibilizer for low-density polyethylene (LDPE)/poly(ethylene terephthalate) (PET) blends was developed. This compatibilizer consists of amine-functionalized PET, which is blended with maleated polyethylene to form a copolymer. The goal is to use this compatibilizer in the future for recycling plastic waste from the marine environment. Fourier-transform infrared spectroscopy confirmed the successful incorporation of amine groups into PET chains through the addition of p-phenylenediamine in a molten state. An increase in diamine content allowed for the visualization of three bands where PET reacted with the diamine. Differential scanning calorimetry suggested that the polyester chains were grafted onto the maleated polyethylene backbone, with crystallinity increasing up to 2.5% diamine content. Scanning electron microscopy (SEM) images showed that the LDPE/PET blend resulted in a continuous polyethylene matrix with a dispersed polyester phase. The blend compatibilized with modified maleated polyethylene, and functionalized PET exhibited an improved interface. Oscillatory rheology and dynamic mechanical analysis indicated that the developed compatibilizer positively impacted the mechanical properties of the compatibilized LDPE/PET blends. This new approach enables the creation of innovative strategies for enhancing the properties of pre-existing polyolefin/polyester recycled blends.

**Keywords:** compatibilization; blends; reactive processing; rheology; recycling

check for updates

Academic Editor: Denis Rodrigue

Received: 17 March 2025
Revised: 16 April 2025
Accepted: 24 April 2025
Published: 1 May 2025

**Citation:** Rodrigues, P.V.; Cestari, S.P.; Cruz, V.; Castro, M.C.R.; Machado, A.V. New Strategy for Upcycling Marine Plastic Waste Through the Development of a Diamine-Functionalized Poly(ethylene terephthalate) Compatibilizer. *Recycling* **2025**, *10*, 82. https://doi.org/10.3390/recycling10030082

**Copyright:** © 2025 by the authors. Licensee MDPI, Basel, Switzerland. This article is an open access article distributed under the terms and conditions of the Creative Commons Attribution (CC BY) license (https://creativecommons.org/licenses/by/4.0/).

## 1. Introduction

Contemporary society is increasingly viewing plastics as a resource rather than as waste. Due to the challenges and costs associated with collecting and sorting post-consumer plastic waste, a more straightforward recycling approach is to bypass these steps by processing mixed plastics with additives that enhance compatibility between different types of polymers. This improvement in the compatibility of heterogeneous plastic blends can facilitate the recycling of unsorted plastics. Caporaso has noted that the poor properties of most polymer blends—resulting from weak molecular forces at the interface of the continuous and dispersed phases—can be strengthened by the addition of copolymers [1–3].

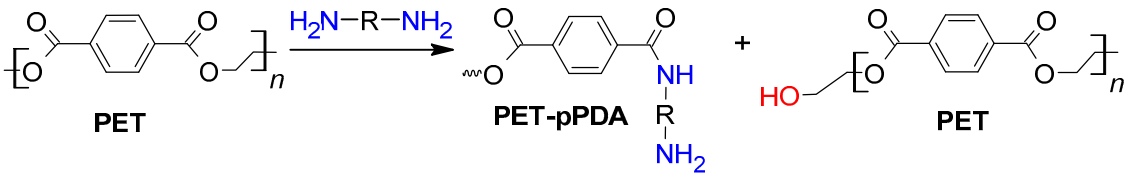
Poly(ethylene terephthalate) (PET) and polyolefins (polyethylene—PE and polypropylene—PP) are the most widely produced polymers globally, accounting for 67% of total production [4]. As stated by Birch, improvements in the compatibilization of PET/PE blends "are extremely desirable for the packaging industry" and can play a crucial role

in promoting the recycling of mixed plastic waste [5,6]. Chen and co-workers have highlighted that this challenge has received attention in the past. While some progress has been made, the compatibilization of PET/polyolefins through the addition of a small amount of polyolefins functionalized with maleic anhydride or glycidyl methacrylate remains insufficient to achieve acceptable properties [7]. The compatibilizers employed are generally based on grafted polyolefins with maleic anhydride or copolymers, such as styrene-ethylene-co-butene-styrene, ethylene-vinyl acetate, and ethylene-methacrylic acid, among others [8–11]. It has been reported that the use of small amounts of these compatibilizers can enhance the mechanical properties of PET/PE systems by altering the fracture mechanism of the PE matrix due to PET phase-induced fibrillation [12]. Additionally, they significantly influence the size of dispersed droplets, resulting in increased strain at break due to the multiblock copolymer localized at the blend's interface [13]. Several commercial compatibilizers are available that are based on polyolefins grafted or copolymerized with polar groups. Tang et al. used some of these compatibilizers to improve compatibility in PET/PE 80/20 systems, highlighting the importance of understanding how polymer chains are spatially arranged in the matrix. Therefore, the effectiveness of each compatibilizer should be evaluated based on all characterized data (mechanical, crystallinity, and morphological), alongside the compatibilizer's molecular location—whether it is predominantly at the interface or dispersed within the bulk [14]. Some commercial nanoclays have also been used to compatibilize blends of PET and PE [15].

Reactive extrusion is a reliable method to enhance the interfacial interaction between immiscible polymers and can be easily adapted to existing extrusion technology. This involves the incorporation of a functionalized material (polymer, monomer, or additive) capable of chemically reacting with one or more components of the blend system during melt processing. It is expected that this reaction develops a grafted or block copolymer at the interface of immiscible phases, improving interfacial adhesion with smaller size particles. Most of the reported works utilize polar groups (such as maleic anhydride, glycidyl methacrylate, and acrylic acid) grafted onto the polyolefin chain as the primary mechanism for compatibilization. In many cases, only the polyester end-groups are able to react with the compatibilizer, or the affinity is enhanced through interactions with carbonyl groups. This limitation restricts the degree of interaction between the two phases [16–19].

Marine-environment plastic waste found on North Portugal beaches primarily consisted of polyolefins and PET from post-consumer products, such as bottles, bags, and caps/lids. This observation aligns with Galgani's 2015 statement [20]. Mechanical recycling of this heterogeneous material would yield an incompatible blend of PET and polyolefins, requiring an effective compatibilizing agent to achieve acceptable properties. Over the last decade, several chemical strategies for PET depolymerization have been reported. Due to their chemical nature, polyesters can be easily modified through organic reactions, such as hydrolysis, aminolysis, reduction, and oxidation by reactive extrusion [21–23]. This process allows for the introduction of reactive functional groups or a change in the sample's polarity, enhancing system reactivity and improving affinity with other materials. Aminolysis is particularly advantageous because of the high reactivity (nucleophilicity) of amine groups, which react more rapidly with PET [24–30]. For example, Todd et al. [31] took advantage of this property by developing a PET-PE multiblock polymer through the aminolysis of PET with amino-telechelic polyethylene via reactive extrusion, significantly improving the mechanical properties of PET/HDPE blends. This approach presents a promising solution to one of the major challenges in plastic recycling, where the traditional separation of immiscible polymers is often impractical. Therefore, this strategy holds great potential for addressing the recycling of mixed plastic waste and enhancing the final properties of recycled plastics, thereby expanding their range of applications.

To address this gap, a compatibilizer was developed by functionalizing PET with 1 wt.% diamine and pre-mixing it with commercial PE-g-MA. Three diamines with different boiling points (ethylenediamine, p-phenylenediamine, and Jeffamine® D-230) were tested, and the one yielding the best functionalization results was selected. Additional blends with 2.5 and 5 wt.% diamine content were prepared to investigate the effect of the diamine on PET structure. The functionalized PET/PE-g-MA blend (Scheme 1) was tested as a compatibilizer in a 50/50 w/w blend of LDPE/PET and compared to a neat PET/PE-g-MA compatibilized blend.




**Scheme 1.** Insertion of an amine group into PET through aminolysis.

## 2. Materials and Methods

### *2.1. Materials*

Poly(ethylene terephthalate) (PET) was kindly provided by Selenis (Ribeira de Nisa, Portugal). Its intrinsic viscosity (IV) measured in dichloroacetic acid at 30 °C (used as received) was 0.79 dL/g, corresponding to an average viscosity molecular weight (Mv) of 25,560 g/mol, calculated using the equation $[M_v] = 67 \times 10^{-4}\ IV^{0.47}$ [32]. Low-density polyethylene (LDPE) LDPE 352E and polyethylene grafted with maleic anhydride (PE-g-MA) Fusabond® E226 were acquired by Dow Chemical (Estarreja, Portugal). PE-g-MA contained between 0.5 and 1 wt.% grafted maleic anhydride. Regarding the diamines, ethylenediamine 99% (EDA) was purchased from Acros Organics (Geel, Belgium), p-phenylenediamine 97% (pPDA) from Alfa Aesar (Karlsruhe, Germany), and Jeffamine® D-230 (jD230) from Huntsman Performance Chemicals (Los Angeles, CA, USA).

### *2.2. PET Functionalization and Specimen Preparation*

Amine-functionalized PETs were prepared using a Haake Rheomix Roller Roters R600 (Thermo Scientific™, Waltham, MA, USA) mixer. First, PET was plasticized for 2 min prior to the addition of diamines. Then, 1 wt.% of each diamine was mixed at 255 °C for 5 min at a rotor speed of 80 rpm. The functionalized PET was designated as PET1%EDA, PET1%pPDA, and PET1%jD230. Before chemical characterization, these materials were purified to remove unreacted reactants. A mixture of trifluoroacetic acid (TFA)/dichloromethane (20/80) was used for this purpose as free p-phenylenediamine dissolves completely in dichloromethane, while non-functionalized PET dissolves in TFA. To assess the effect of the diamine on PET chemical structure and crystallinity, two additional pPDA–functionalized PETs (PET2.5%pPDA and PET5%pPDA) were produced.

Specimens for parallel plate rheology and dynamic mechanical analysis, with a thickness of approximately 1 mm, were prepared by compression molding in a heated press at 270 °C and 4.8 MPa for 5 min, followed by cooling in the press at 25 °C and 4.8 MPa for an additional 5 min.

### *2.3. Compatibilization of LDPE/PET Blend*

Blends were processed under the same temperature and time conditions as PET functionalization, with the rotor speed increased to 100 rpm to enhance the mixing of the incompatible polymers (PET and LDPE). First, the compatibilizers were prepared by blending neat PET and pPDA–functionalized PET with PE-g-MA in a 50/50 ratio—Cpt1

(PET/MAPE) and Cpt2 (PET1%pPDA/MAPE). Next, 9 wt.% of each compatibilizer was added together with a 50/50 blend of PET and LDPE, and the results were compared to those of the pure blend and the parent materials.

### *2.4. Characterization*

#### 2.4.1. Fourier-Transform Infrared Spectroscopy (FTIR)

Room temperature FTIR spectra were acquired using a 4100 Jasco spectrometer (Jasco, Easton, MD, USA) in transmittance mode with the following parameters: 32 scans/min, 4 $cm^{-1}$ resolution, and a range of 4500–400 $cm^{-1}$. Thin films of all experiments were prepared by compression molding in a hot press at 270 °C under a pressure of 7.7 MPa.

#### 2.4.2. Differential Scanning Calorimetry (DSC)

DSC analysis was performed using Netzsch DSC 200 F3 (Netzsch, Selb, Germany) equipment. The samples were analyzed under a nitrogen atmosphere, following ASTM D3418 [33]. In the first cycle, the sample was heated from 0 to 270 °C at a rate of 10 °C·$min^{-1}$ and held at 270 °C for 1 min. The second cycle involved cooling at the same rate of 10 °C·$min^{-1}$ until reaching 0 °C. Then, a third cycle was repeated in the same conditions as the first cycle. The crystallization temperature (*Tc*) was obtained from the second cycle, while the crystalline melting temperature (*Tm*) and degree of crystallinity (*Xc*) of PET were obtained from the third cycle. The *Xc* was determined based on the ratio of the melting enthalpy ($\Delta Hm$) of PET to that of 100% crystalline PET (140 J·$g^{-1}$) [34,35].

#### 2.4.3. Thermogravimetric Analysis (TGA)

Thermogravimetric evaluation was performed using a TA Q500 model (TA Instruments, New Castle, DE, USA) at a temperature range from 40 °C to 600 °C and a rate of 10 °C·$min^{-1}$, and under a nitrogen flow of 60 mL·$min^{-1}$. Parameters such as mass loss at the initial (*Tonset*), maximum speed (*Tmax*), and final degradation temperatures (*Tfinal*), and residue content were measured.

#### 2.4.4. Rheological Measurements

Rheology was conducted using a stress-controlled rheometer MCR-302 (Anton Paar, Graz, Austria) equipped with a heating chamber. Samples were placed in a 25 mm diameter parallel-plate geometry at a typical gap distance of 1 mm. Oscillatory frequency sweeps were performed from 0.01 to 100 Hz at 280 °C within a linear regime to assess viscoelastic properties (storage modulus—*G*′, loss modulus—*G*″, and complex viscosity—$\eta^*$).

#### 2.4.5. Dynamic Mechanical Analysis (DMA)

DMA tension measurements of the materials were conducted using a dynamic mechanical analyzer TT-DMA TRITON (LabWrench, Midland, ON, Canada) at a frequency of 1 Hz. The films (20 × 3 × 0.2 mm) were assessed with a normal force of 1 N over a temperature range of 30 °C to 110 °C and at a rate of 2 °C·$min^{-1}$ to access the storage modulus—*E*′ and Tan Delta.

#### 2.4.6. Field Emission Gun-Scanning Electron Microscopy (FEG-SEM)

Morphological investigation was achieved using an ultra-high resolution Field Emission Gun-Scanning Electron Microscope (FEG-SEM), NOVA 200 Nano SEM (FEI Company, Hillsboro, Oregon, EUA). All the samples were previously fractured in liquid nitrogen and coated with a thin film (2 nm) of Au-Pd (80–20 weight %) in a high-resolution sputter coater (208HR, Cressington Company, Watford, UK).

## 3. Results and Discussion

In the FTIR spectra of neat and amine-functionalized PET (Figure 1), we observe the characteristic bands of PET: the 3100–2900 $cm^{-1}$ range, attributed to aromatic and aliphatic -C-H bond stretching; around 1730 $cm^{-1}$ for carbonyl ester bond stretching; approximately 1300 $cm^{-1}$ for ester group stretching; and around 1100 $cm^{-1}$ for the methylene group. Furthermore, the results indicate that only pPDA affects the chemical structure of PET as the PET1%pPDA spectrum reveals two new bands around 3380 and 1515 $cm^{-1}$, which are associated with the axial and weak angular deformation of the N–H stretch in amines and secondary amides, respectively.

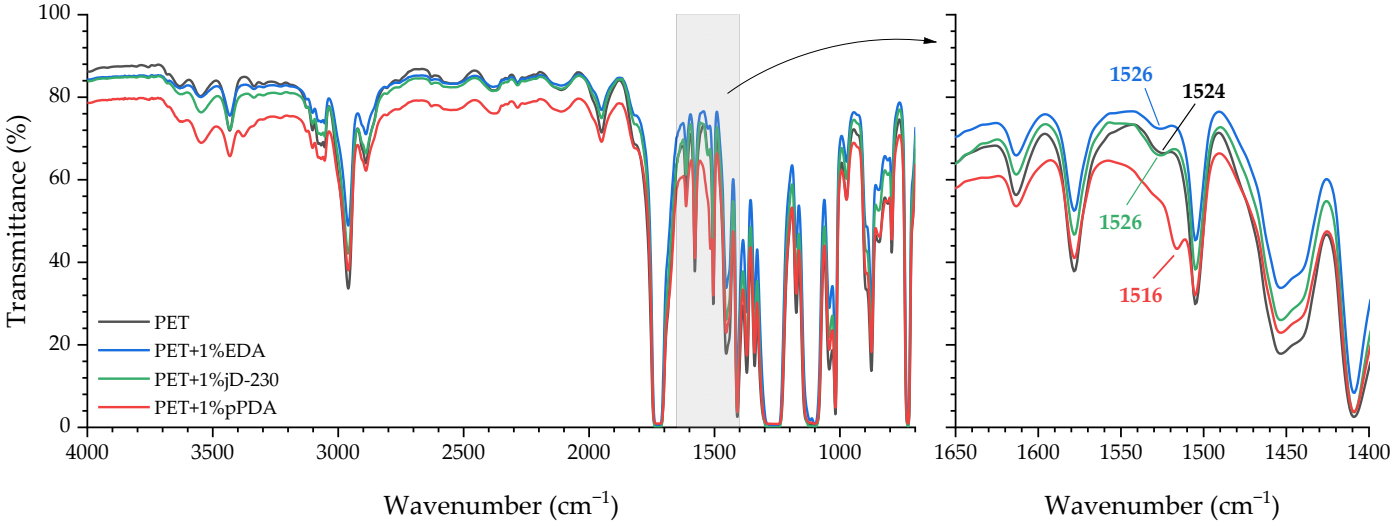



**Figure 1.** FTIR spectra of neat PET and amine functionalized PET.

Increasing the pPDA content to 2.5 and 5 wt.% (Figure 2) results in significant changes in the 1515, 1675, and 3380 $cm^{-1}$ bands, all related to amide stretching. The band around 1675 $cm^{-1}$, assigned to the axial deformation of C=O double bonds in N–substituted amides, becomes noticeable at higher pPDA concentrations due to the overlap with carbonyl ester bond stretching around 1730 $cm^{-1}$ [36].

Figure 3 and Table 1 present DSC data for amine-functionalized PETs. With the exception of pPDA, the diamines resulted in a slight increase in the Tg of the samples, indicating limited mobility restriction during the glassy–rubbery transition. The most significant increase in the crystallinity (Xc) of PET, approximately 15%, was observed at 2.5 wt.% of pPDA. This enhancement can be attributed to an improved crystalline arrangement of PET's crystallizable portions following chain scission induced by this amount of diamine [37].

**Table 1.** DSC data and $X_c$ of the amine-functionalized PETs.

| Material | $T_g$ (°C) | $T_{m1}$ (°C) | $T_{m2}$ (°C) | $\Delta H_m$ ($J \cdot g^{-1}$) | $X_c$ (%) |
|---|---|---|---|---|---|
| PET | 82 | 240 | 246 | 37 | 26 |
| PET+1%EDA | 85 | 242 | 249 | 35 | 25 |
| PET+1%pPDA | 81 | 241 | 249 | 40 | 29 |
| PET+2.5%pPDA | 90 | 228 | 244 | 42 | 30 |
| PET+5%pPDA | 84 | 220 | 230 | 38 | 27 |
| PET+1%jD230 | 83 | 240 | 248 | 41 | 29 |

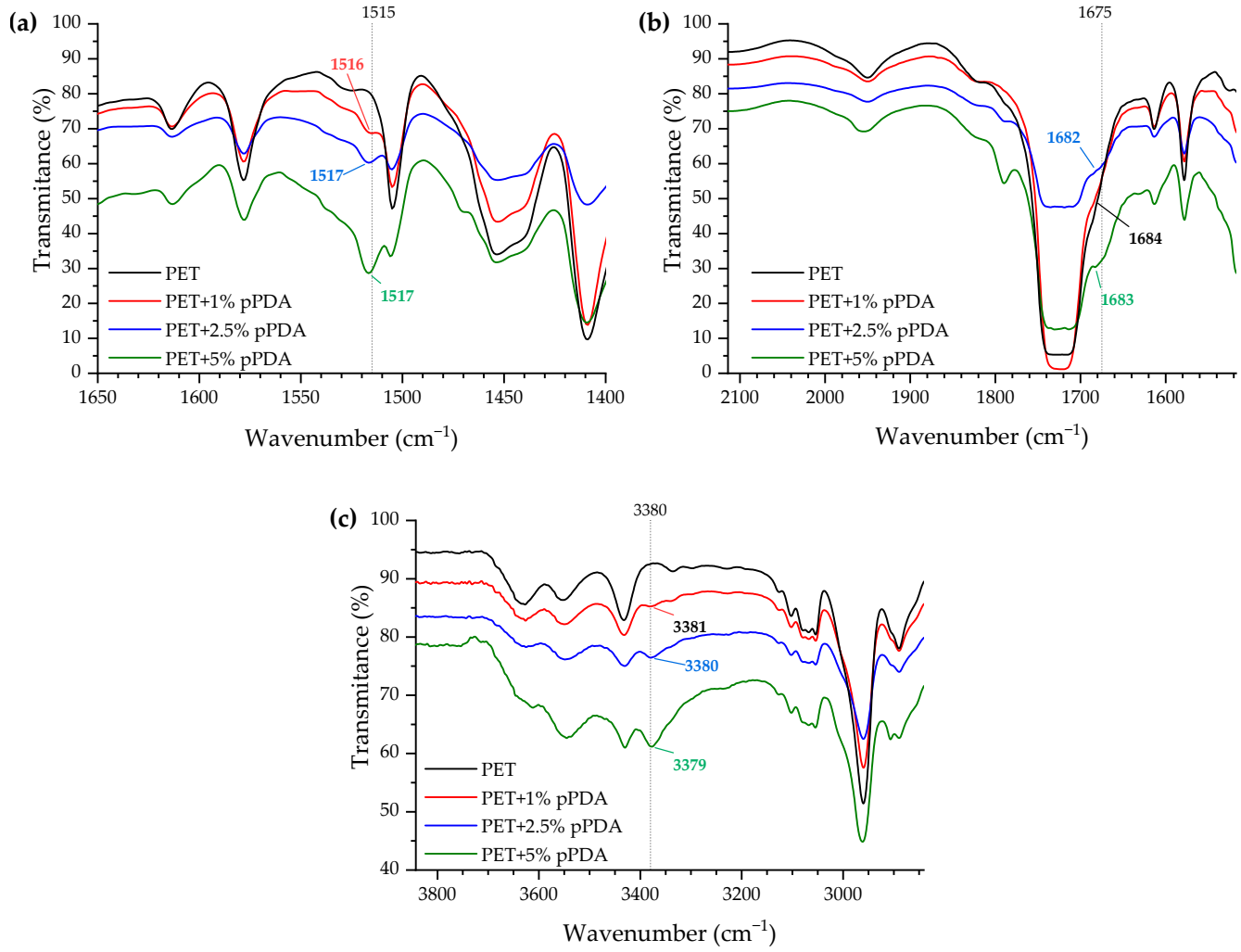



**Figure 2.** FTIR spectra of neat PET and pPDA–functionalized PET around 1515 cm$^{-1}$ (**a**), 1675 cm$^{-1}$ (**b**), and 3380 cm$^{-1}$ (**c**) bands.

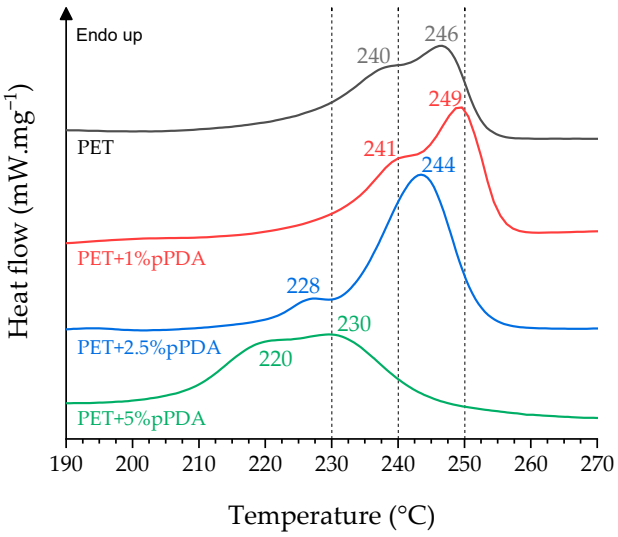



**Figure 3.** DSC curves of neat PET and pPDA–functionalized PETs.

The melting temperatures for PET+5% pPDA and PET+1% pPDA range from 220 to 250 °C, respectively. The addition of 1 wt.% pPDA raises the melting temperature to 250 °C, which is linked to a different crystal organization. The sample with 2.5 wt.% pPDA

exhibited higher crystallinity at 240 °C but eliminated the melting peak around 250 °C. These changes can be attributed to a reduction in the polymer's molecular weight caused by aminolysis, which favors the formation of smaller, less stable crystals that melt at lower temperatures [37]. The chain scission that occurs when 5% pPDA is used eliminated both the 240 °C and 250 °C populations.

Both PET and LDPE (Table 2) exhibited characteristic thermal transitions: PET $T_g$ 82 °C, Tc 187 °C, and Tm 246 °C, and LDPE Tc 96 °C, and Tm 116 °C (Table 3). The calorimetric data for PE-g-MA were similar to those of LDPE but with a lower degree of crystallinity (Xc) of 23%.

**Table 2.** DSC data of the materials.

| Material | LDPE Fraction | | | | PET Fraction | | | | |
|---|---|---|---|---|---|---|---|---|---|
| | $T_m$ (°C) | $T_c$ (°C) | $\Delta H_m$ (J·g$^{-1}$) | $X_c$ (%) | $T_m$ (°C) | $T_c$ (°C) | $T_g$ (°C) | $\Delta H_m$ (J·g$^{-1}$) | $X_c$ (%) |
| PET | - | - | - | - | 240/246 | 187 | 82 | 37 | 26 |
| LDPE | 116 | 96 | 115 | 39 | - | - | - | - | - |
| LDPE/PET | 109 | 96 | 64 | 22 | 242/249 | 194 | - | 16 | 11 |
| LDPE/PET+9%Cpt1 | 114 | 100 | 64 | 22 | -/247 | 210 | - | 15 | 11 |
| LDPE/PET+9%Cpt2 | 108 | 98 | 62 | 21 | -/249 | 184 | - | 19 | 13 |
| MAPE | 122 | 100 | 68 | 23 | - | - | - | - | - |
| Cpt1 | 120 | 104 | 64 | 22 | -/250 | 213 | - | 20 | 15 |
| Cpt2 | 120 | 103 | 64 | 22 | -/249 | 192 | - | 19 | 14 |

**Table 3.** TGA data of the aminolyzed PETs.

| Material | $T_{onset}$ (°C) | $T_{max}$ (°C) | $T_{final}$ (°C) | Residue (%) |
|---|---|---|---|---|
| PET | 404 | 430 | 500 | 0 |
| PET+1%pPDA | 409 | 436 | 500 | 14 |
| PET+2.5%pPDA | 407 | 435 | 500 | 13 |
| PET+5%pPDA | 404 | 432 | 500 | 17 |
| pPDA | 153 | 177 | 200 | 1 |

During the crystallization step, the PET/PE-g-MA compatibilizer displayed two peaks corresponding to the parent materials. The PET moiety exhibited a 26 °C increase in Tc. The degree of crystallinity of PE-g-MA remained nearly constant, while the Xc of PET decreased by approximately 42%. This behavior indicates that the PE-g-MA structure was preserved, while PET chains were grafted onto the PE-g-MA structure in regions functionalized with maleic anhydride through amide and/or ester bonds [38]. The calorimetric characteristics of the compatibilizer Cpt2 were similar to those of Cpt1, except for a slight increase in PET's Tc (only 5 °C). This difference in Tcs suggests that in Cpt2, the functionalized PET chains may have reacted at both end-groups with the maleic anhydride of PE-g-MA and another PET chain end-group, forming longer chains and larger crystals that are packed at lower temperatures (192 °C).

Regarding the blends, both LDPE and PET moieties exhibited crystallinity (Xc) lower than that of the parent materials across all blends. The reduction was between 44 and 46% for LDPE and 49–58% for PET. The overlay of the melting and crystallization peaks of the LDPE and PET portions (see Figure 4) indicated that the LDPE/PET peaks resemble shapes of the peaks of the pure polymers, although with lower enthalpies and at different temperatures. The LDPE region of the LDPE/PET blend showed a 44% decrease in crystallinity, while the blend displayed the crystallization events of both polymers. The PET $T_c$ increased

to 194 °C, while LDPE exhibited a peak at 60 °C and a second peak at 96 °C. Since the PET portion crystallized first (at 194 °C), the movement of LDPE chains toward crystallization centers was hindered, impairing crystal growth due to steric hindrance. The peak in the PET melting region was less intense (by 57%) but occurred at slightly higher temperatures. The Tc peak of the blend, occurring at 194 °C before the neat PET peak at 187 °C, indicates that smaller, less perfect crystals were formed.

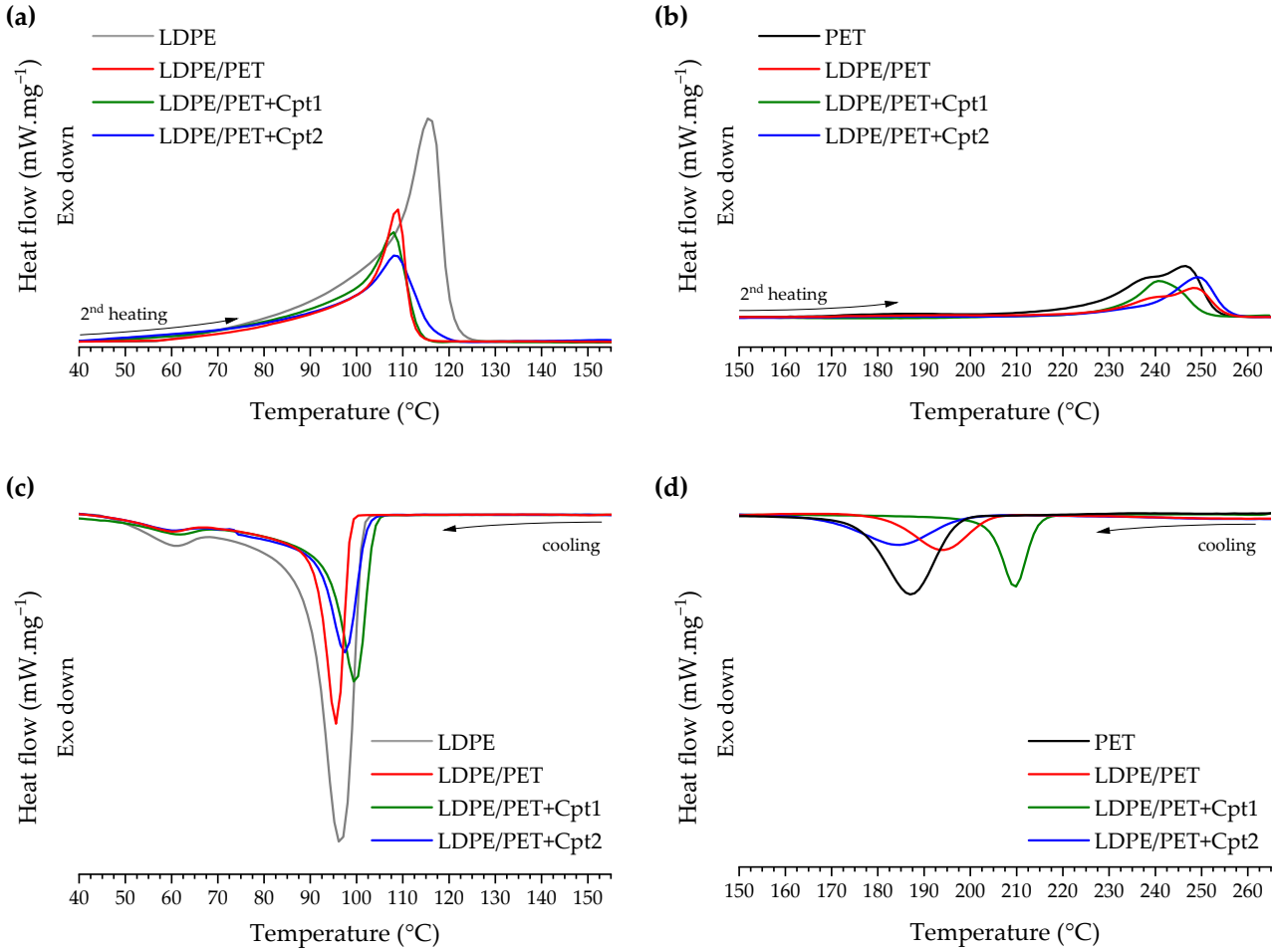



**Figure 4.** Melting and crystallization peaks of blends in the LDPE region (**a**,**c**) and PET region (**b**,**d**).

In the LDPE/PET+9%Cpt1 blend, the LDPE component melted similarly to the pure blend, with a slightly different Tm and Tc (+5 °C and −6 °C, respectively). This behavior indicates the formation of more perfect crystals that crystallized later and melted at higher temperatures. The PET phase showed only one peak, suggesting that crystallization in the 240 °C range was enhanced. The melting enthalpy was similar to that of the pure blend, but the Tc occurred earlier (210 °C), indicating that these crystals were smaller and less perfect. This may have resulted from PET grafting onto the PE-g-MA backbone through end-group interchange reactions [38], which could have reduced the polymer's ability to undergo primary crystallization. The crystal population below 220 °C appeared to have disappeared.

For the LDPE/PET+9%Cpt2 blend, the LDPE portion showed a 2 °C increase in Tc, while Tm and Xc were slightly lower, indicating that amine-functionalized PET negatively affected the crystallization conditions of LDPE. In the PET phase, a single melting peak primarily appeared around 250 °C and crystallization occurred in the same temperature range as neat PET (approximately 185 °C). Amine-functionalized PET in Cpt2 appeared to have reacted with the PET phase of the blend (Scheme 1), replicating the crystal perfection

and increased crystallinity. This effect is attributed to a reduction in PET molar weight due to aminolysis and heterogeneous nucleation by-products from aminolysis. Additionally, both polymers used in this research may contain catalytic residues that influenced their crystallization during the solidification process. The synthesis of LDPE typically uses a titanium-based catalyst, while PET employs a catalyst or a mixture of catalysts based on antimony and others. Increases in the Tcs of the compatibilized blends may also result from the heterogeneous nucleation of PET and LDPE chains induced by these catalytic residues.

The thermogravimetric (TG) and derivative thermogravimetric (DTG) curves of PET, pPDA, and pPDA–functionalized materials (Figure 5 and Table 3) indicate that no unreacted pPDA was present in the modified PETs. All pPDA contents exhibited a first degradation step between 250 and 310 °C, which is associated with the degradation of aminolysis volatile elements [24]. However, this did not significantly affect the thermal stability of the polymer up to the selected processing temperature of 255 °C. The residue content increased with higher diamine content, which can be attributed to char formation [39].

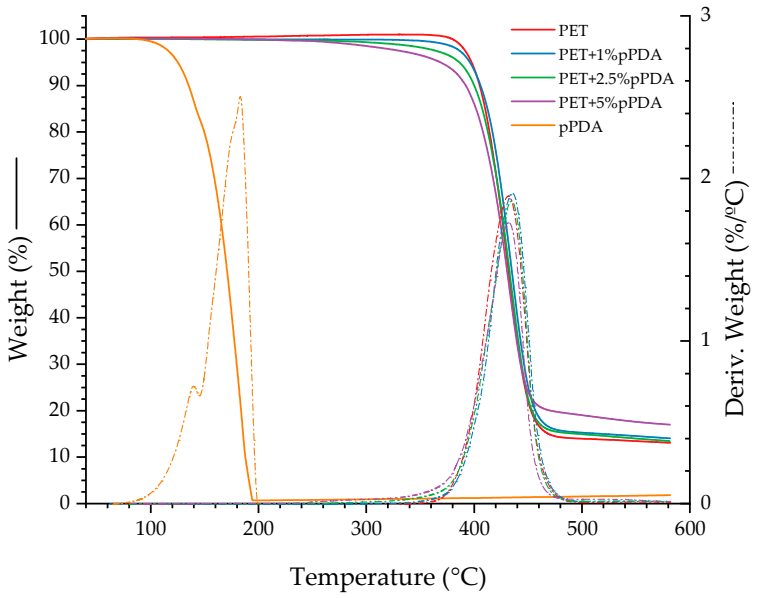
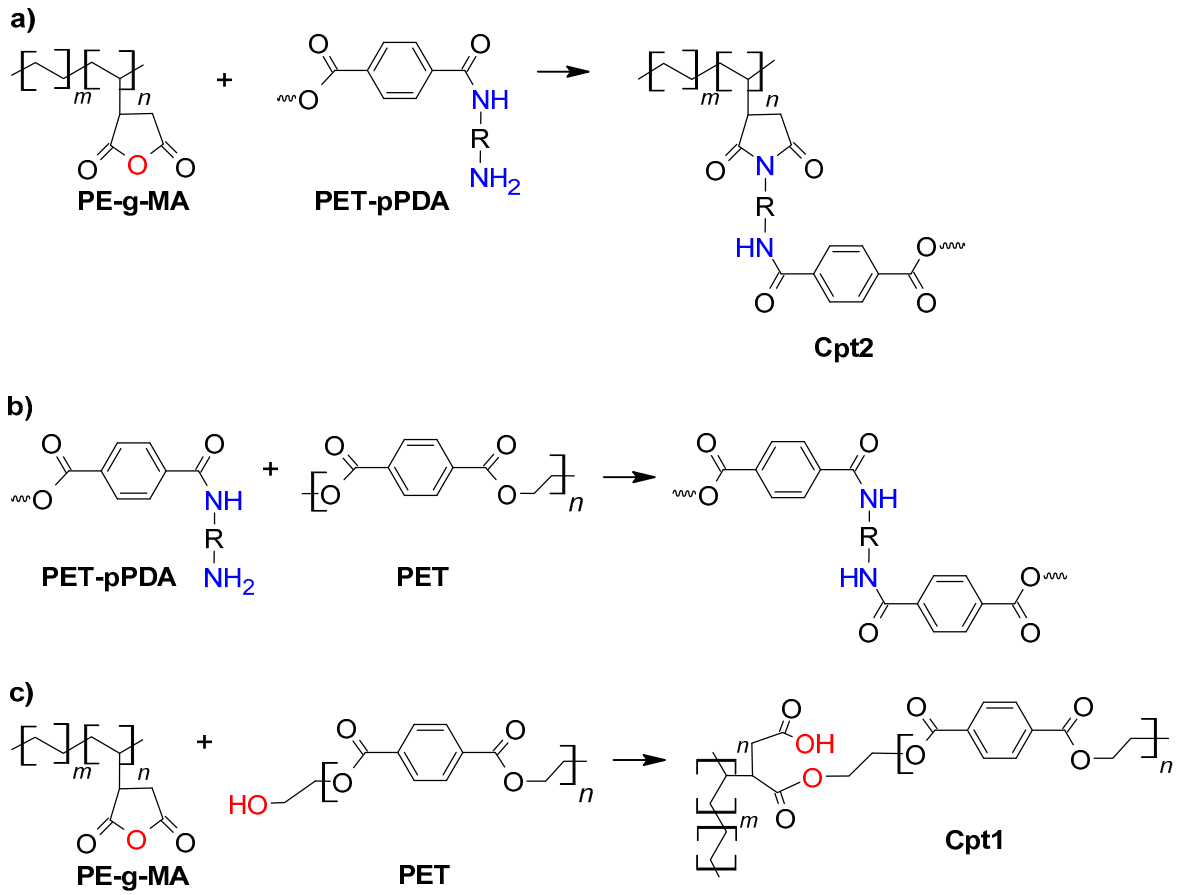



**Figure 5.** TGA curves of neat PET and pPDA–functionalized PETs.

According to the previously discussed data, Scheme 2 illustrates the expected reactions between amine-functionalized PET and PE-g-MA. Several authors have reported that PET aminolysis primarily produces terephthalamide derivatives [24–26]. In this study, we assumed that PET aminolysis results in half of the aminolyzed PET chains containing an amine end-group (PET-pPDA), while the other half consists of shorter PET chains. The free amine end-group in the PET-pPDA structures could react with the anhydride group present in PE-g-MA, originating Cpt2 with imide groups (Scheme 2a), or with other PET chains, once more, during the aminolysis phenomenon (Scheme 2b). Additionally, the PET hydroxyl end-group could react with the anhydride grafted in the PE-g-MA chain, originating Cpt1, through a new ester linkage (Scheme 2c).

Rheological parameters (Figure 6) were obtained within the linear viscoelastic region. The complex viscosity curves indicated that PET behavior remained unchanged as the frequency increased up to 100 Hz, exhibiting lower viscosity compared to the other materials. The LDPE/PET blend demonstrated shear-thinning behavior, characterized by a sharp decrease in complex viscosity with increasing frequency. The addition of Cpt1 and Cpt2 significantly altered the rheological properties of the incompatible blend; the increase in viscosity with the addition of Cpt1 and Cpt2 may be attributed to enhanced interfacial

adhesion resulting from in situ compatibilizer formation. However, the flow conditions during measurement likely also affect the morphology of the dispersed phase. At lower shear rates, the viscosity of the blends is comparable to that of LDPE. Both the storage and loss modulus of the incompatible and compatibilized blends exhibit similar trends, with the compatibilized blends showing higher values that resemble those of LDPE.




**Scheme 2.** Possible chemical reactions between (**a**) PET-pPDA and PE-g-MA, (**b**) PET-pPDA and PET, and (**c**) PET and PE-g-MA.

SEM micrographs reveal a continuous LDPE phase with dispersed PET droplets. The LDPE/PET blend (Figure 7a) displays the PET phase as spheres and cylinders within the LDPE matrix, characterized by poor interfacial adhesion, typical of a non-compatible blend. In contrast, both compatibilized blends show distinct morphologies with more homogeneous dispersion and smaller droplets. Although smaller, some PET droplets in the LDPE/PET+9%Cpt1 blend are detached from the LDPE matrix (green circle in Figure 7b), indicating poor adhesion between the phases. The smallest droplets are observed in the LDPE/PET+9%Cpt2 blend, which demonstrates the lowest interfacial tension between PET and LDPE (red circle in Figure 7c, showing a fractured PET phase without debonding). This behavior can be attributed to the reaction between the MA groups of PE-g-MA and functionalized PET, resulting in a copolymer at the interface.

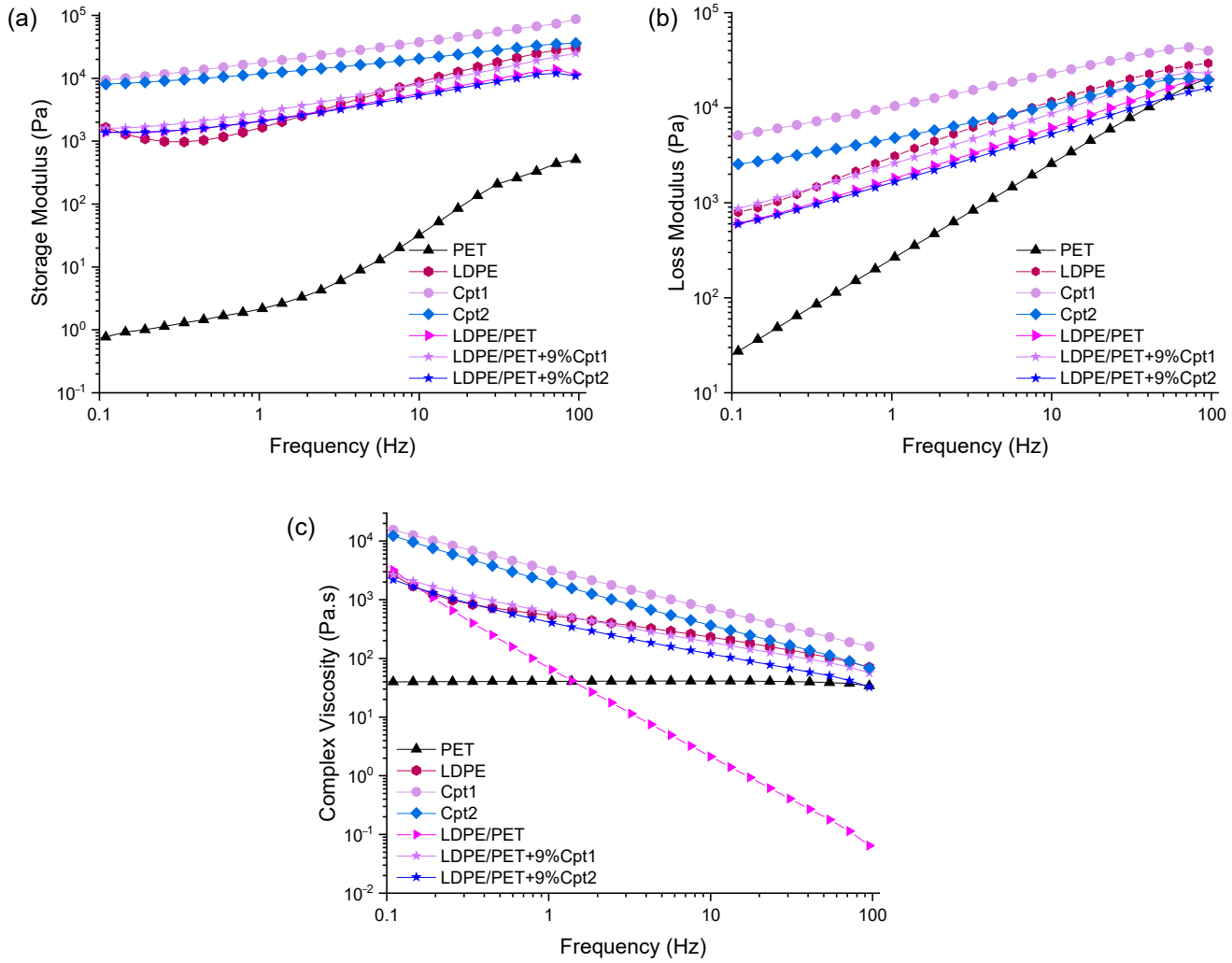



**Figure 6.** Storage modulus (**a**), loss modulus (**b**), and complex viscosity (**c**).

DMA analysis of the materials is displayed in Figures 8 and 9, and Table 4. Comparing both compatibilizers (Figure 8), Cpt2 exhibits a slightly higher E′ than Cpt1, which can be attributed to the chemical reaction between the functionalized PET and MA groups. No significant decrease is observed after 80 °C due to the $T_g$ of PET. Among the two polymers, PET shows the highest storage modulus at 30 °C–E′$_{30°C}$- (above 1.5 GPa), while LDPE presents the lowest, around 231 MPa. For the blends, LDPE/PET has the lowest E′ value, whereas the compatibilized blends have E′ values situated between those of the individual components, indicating the effectiveness of the compatibilizers. The E′ of LDPE/PET+9%Cpt2 (822 MPa) is 40% higher than that of LDPE/PET+9%Cpt1 (587 MPa). The elastic contribution of the compatibilized blends above the PET $T_g$ reveals higher values than those of the remaining samples.

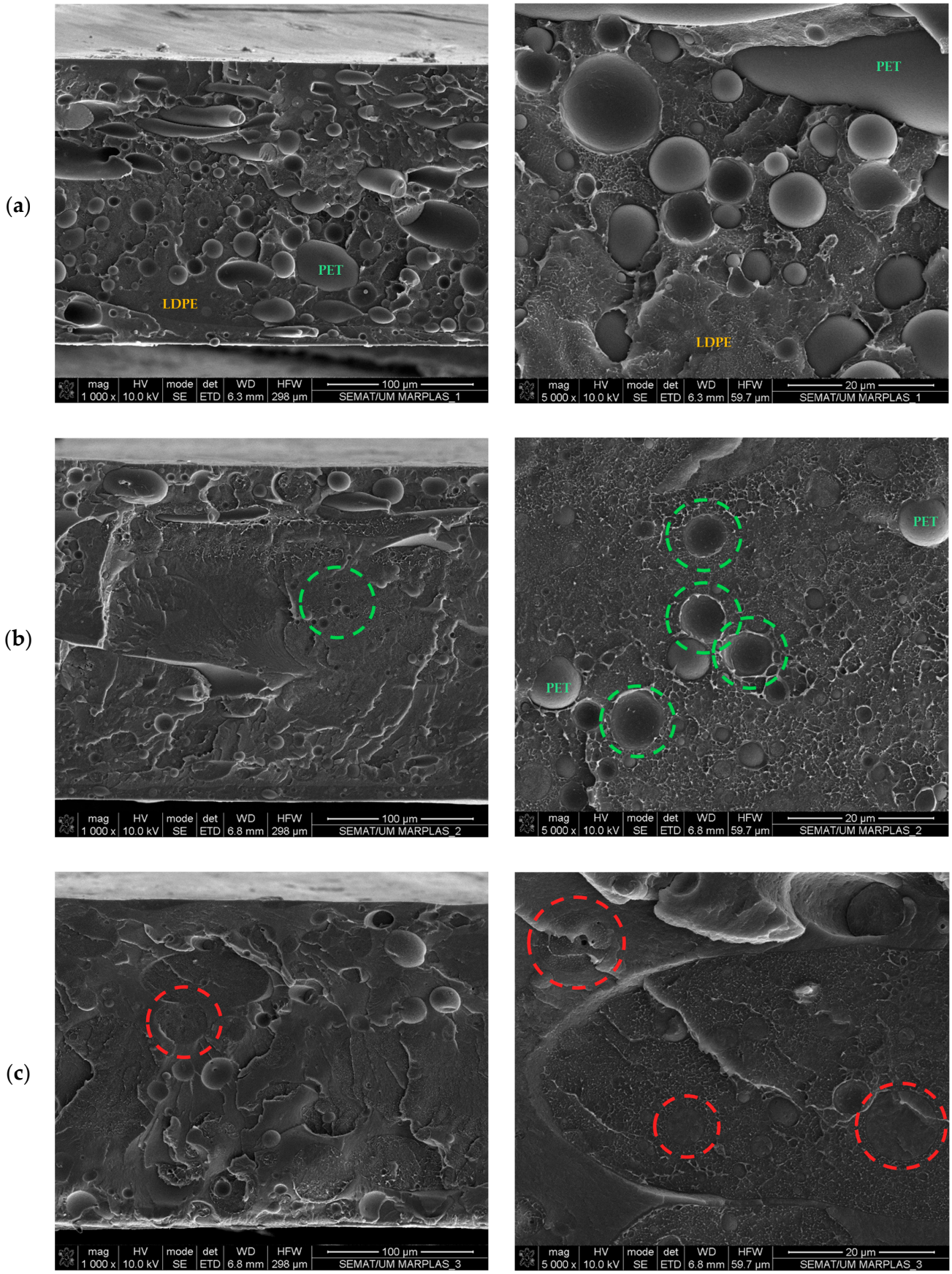



**Figure 7.** FEG-SEM images at 1000× (**left**) and 5000× (**right**): (**a**) PET-LDPE; (**b**) LDPE/PET+9%Cpt1, and (**c**) LDPE/PET+9%Cpt2. Green and red circles indicate the PET phase dispersed in LDPE using distinct compatibilizers.

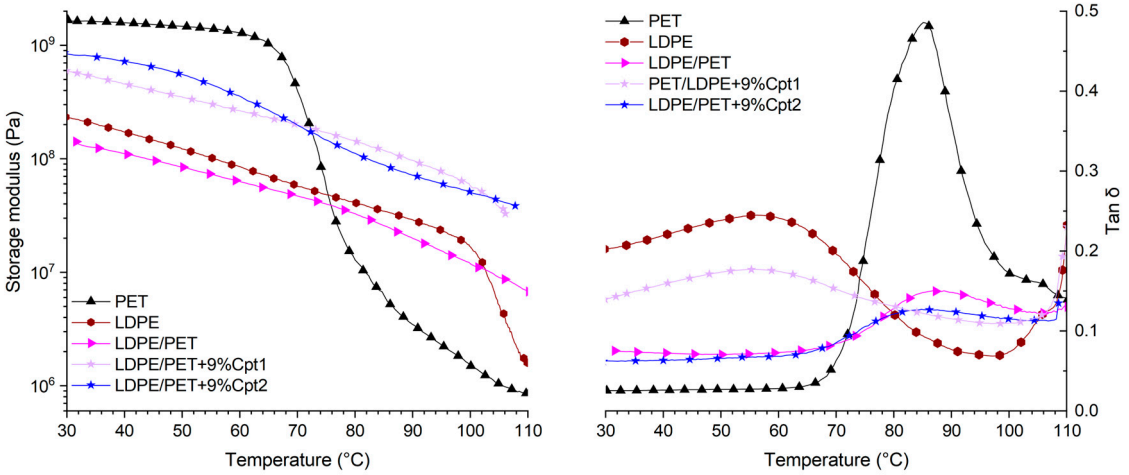



**Figure 8.** DMA curves of neat PET, LDPE, and blends: storage modulus (**left**) and Tan Delta (**right**).

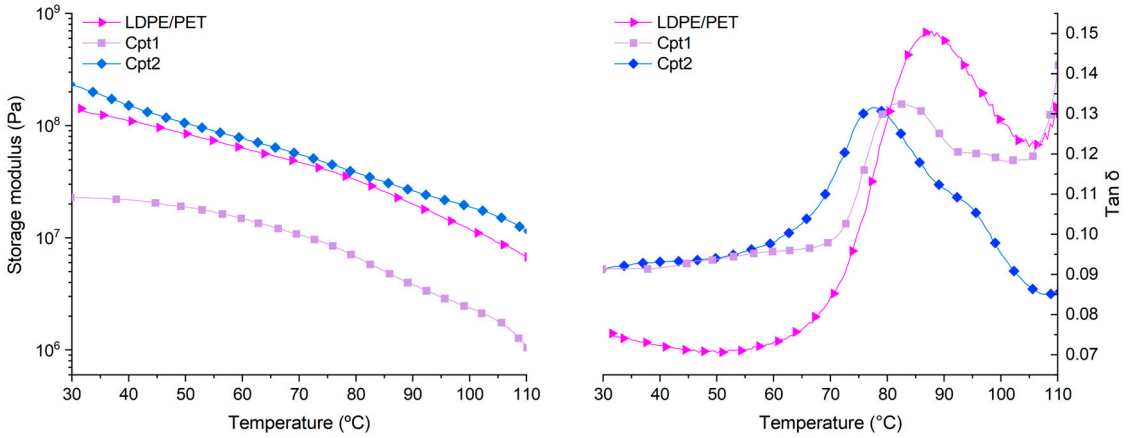



**Figure 9.** DMA analysis of compatibilizer Cpt1 and Cpt2, and LDPE/PET blend.

**Table 4.** Storage modulus (at 30 and 100 °C), $T_g$, and damping factor of neat polymers, blends, and compatibilizers.

| Material | $E'_{30°C}$ (MPa) | $E'_{100°C}$ (MPa) | $T_g$ *at* tan δ peak (°C) | Tan δ |
|---|---|---|---|---|
| PET | 1636.8 | 1.5 | 85.1 | 0.486 |
| LDPE | 231.3 | 18.4 | - | - |
| LDPE/PET | 141.0 | 11.8 | 86.8 | 0.151 |
| LDPE/PET+9%Cpt1 | 587.2 | 56.3 | - | - |
| LDPE/PET+9%Cpt2 | 822.0 | 49.9 | 84.8 | 0.127 |
| Cpt1 | 22.9 | 2.3 | 82.0 | 0.132 |
| Cpt2 | 233.6 | 18.6 | 77.3 | 0.131 |

The Tan δ curves of the samples also display profiles dependent on the presence of the compatibilizer. While the PET $T_g$ appears between 80 and 90 °C, the α-relaxation of LDPE is observed between 40 and 70 °C. Blending PET with LDPE decreases the damping factor of PET while maintaining the same peak value as neat PET at 85 °C. The development of the compatibilizers has shifted the $T_g$ to lower values, which is more pronounced for Cpt2 (77 °C) than for Cpt1 (82 °C). This indicates better interfacial adhesion between the PET and LDPE phases in agreement with rheological and SEM results.

## 4. Conclusions

Among the studied diamines and reaction conditions, p-phenylenediamine (pPDA) proved to be the most effective in incorporating amine and/or amide groups into the

PET chains. This functionalization was confirmed by FTIR spectroscopy, which revealed new absorption bands at 3380, 1675, and 1515 $cm^{-1}$ corresponding to N–H stretching vibrations. Thermogravimetric analysis indicated complete reaction of pPDA, with no residual unreacted diamine, and showed no significant reduction in PET's thermal stability up to its average processing temperature (270 °C).

Differential scanning calorimetry results highlighted a clear difference in crystallization temperatures (Tc) between the Cpt1 and Cpt2 compatibilizers. These findings suggest that the functionalized PET chains were successfully grafted onto the PE-g-MA backbone. In the Cpt2 compatibilizer, amine-functionalized PET appeared to react both with PE-g-MA and with other PET chain end-groups, resulting in longer chains and larger crystals, reflected in a lower glass transition temperature (Tg). Calorimetric data showed that using PE-g-MA alone improved the crystallinity of the LDPE phase, while incorporating amine-functionalized PET significantly enhanced the crystallinity of the PET phase.

Rheological, SEM, and DMA analyses confirmed that both compatibilizers improved interfacial adhesion in the LDPE/PET blend. While the LDPE/PET+9%Cpt2 blend demonstrated a slightly higher storage modulus at room temperature, both compatibilizers performed comparably in enhancing the blend's interface. In summary, PE-g-MA is better suited to improve LDPE crystallinity, whereas pre-mixing PE-g-MA with amine-functionalized PET is more effective at enhancing PET crystallinity. The choice between these strategies should be guided by the specific mechanical and thermal requirements of the target application.

The findings demonstrate the potential for tailoring LDPE/PET blends through strategic compatibilization to achieve enhanced material properties. However, scaling up this approach poses several challenges. The use of aromatic diamines such as pPDA may introduce cost and sourcing constraints, as well as potential environmental and health concerns due to their toxicity and reactivity. Processing conditions must also be tightly controlled to avoid degradation or incomplete reactions during extrusion. Moreover, ensuring uniform dispersion and optimal reaction between PET and compatibilizers at an industrial scale may require specialized equipment or additional processing steps. These factors must be carefully evaluated when translating laboratory-scale success into viable commercial applications.

**Author Contributions:** Conceptualization, S.P.C., P.V.R. and A.V.M.; methodology, S.P.C., P.V.R., M.C.R.C. and A.V.M.; validation, S.P.C. and A.V.M.; formal analysis, S.P.C.; investigation, S.P.C., P.V.R., V.C. and M.C.R.C.; resources, A.V.M.; data curation, S.P.C., P.V.R., M.C.R.C. and A.V.M.; writing—original draft preparation, S.P.C.; writing—review and editing, P.V.R., M.C.R.C. and A.V.M.; visualization, S.P.C., P.V.R., M.C.R.C. and A.V.M.; supervision, A.V.M.; project administration, A.V.M.; funding acquisition, A.V.M. All authors have read and agreed to the published version of the manuscript.

**Funding:** This work was funded by the CCDR-N-North Portugal Regional Coordination and Development Commission under the scope of Programa Operacional Regional do Norte 2014–2020 | NORTE 2020-MarPlas project (Ref. NORTE01-0145-FEDER-000080).

**Data Availability Statement:** The raw/processed data required to reproduce these findings cannot be shared at this time as the data also form part of an ongoing study.

**Acknowledgments:** The authors thank the Sistema de Apoio à Investigação Científica e Tecnológica-"Projetos Estruturados de I&D&I"-HORIZONTE EUROPA, reference: NORTE-01-0145-FEDER-000080 for financially supporting the Universidade do Minho's "Evaluation and valorisation of plastics and microplastics in marine environment–MarPlas" Project, within which this research was developed.

**Conflicts of Interest:** The authors declare no conflicts of interest. The funders had no role in the design of the study; in the collection, analyses, or interpretation of data; in the writing of the manuscript; or in the decision to publish the results.

## References


1. Kučera, F.; Petruš, J.; Žídek, J.; Poláček, P.; Šimonek, M. An Approach on Reactive Processing of Plastic Waste. *Polym. Eng. Sci.* **2022**, *62*, 4100–4114. [CrossRef]
2. Schyns, Z.O.G.; Shaver, M.P. Mechanical Recycling of Packaging Plastics: A Review. *Macromol. Rapid Commun.* **2021**, *42*, 2000415. [CrossRef] [PubMed]
3. Caporaso, L.; Iudici, N.; Oliva, L. Synthesis of Well-Defined Polypropylene-Graft-Polystyrene and Relationship between Structure and the Ability to Compatibilize the Polymeric Blends. *Macromolecules* **2005**, *38*, 4894–4900. [CrossRef]
4. Geyer, R.; Jambeck, J.R.; Law, K.L. Production, Use, and Fate of All Plastics Ever Made. *Sci. Adv.* **2017**, *3*, e1700782. [CrossRef] [PubMed]
5. Birch, N.P.; Liu, K.; Mun, S.C.; Ghazaryan, G.; Senger, C.T.; Ellison, C.J.; Macosko, C.W.; Peterson, T.H.; Mukhopadhyay, S.; Thurber, C.M. Accelerating the Coupling of Maleated Polyolefins with Polyesters via Tin Compounds. *Macromolecules* **2019**, *52*, 8359–8366. [CrossRef]
6. Champagne, M.F.; Huneault, M.A.; Roux, C.; Peyrel, W. Reactive Compatibilization of Polypropylene/Polyethylene Terephthalate Blends. *Polym. Eng. Sci.* **1999**, *39*, 976–984. [CrossRef]
7. Chen, S.-C.; Zhang, L.-H.; Zhang, G.; Zhong, G.-C.; Li, J.; Zhang, X.-M.; Chen, W.-X. An Investigation and Comparison of the Blending of LDPE and PP with Different Intrinsic Viscosities of PET. *Polymers* **2018**, *10*, 147. [CrossRef] [PubMed]
8. Kalfoglou, N.K.; Skafidas, D.S.; Kallitsis, J.K.; Lambert, J.-C.; Van der Stappen, L. Comparison of Compatibilizer Effectiveness for PET/HDPE Blends. *Polymer* **1995**, *36*, 4453–4462. [CrossRef]
9. Maris, J.; Bourdon, S.; Brossard, J.-M.; Cauret, L.; Fontaine, L.; Montembault, V. Mechanical Recycling: Compatibilization of Mixed Thermoplastic Wastes. *Polym. Degrad. Stab.* **2018**, *147*, 245–266. [CrossRef]
10. Zhang, Y.; Zhang, H.; Guo, W.; Wu, C. Effects of Different Types of Polyethylene on the Morphology and Properties of Recycled Poly(Ethylene Terephthalate)/Polyethylene Compatibilized Blends. *Polym. Adv. Technol.* **2011**, *22*, 1851–1858. [CrossRef]
11. Ha, C.-S.; Park, H.-D.; Kim, Y.; Kwon, S.-K.; Cho, W.-J. Compatibilizer in Polymer Blends for the Recycling of Plastics Waste I: Preliminary Studies on 50/50 Wt% Virgin Polyblends. *Polym. Adv. Technol.* **1996**, *7*, 483–492. [CrossRef]
12. Fasce, L.; Seltzer, R.; Frontini, P.; Pita, V.J.R.; Pacheco, E.B.A.V.; Dias, M.L. Mechanical and Fracture Characterization of 50:50 HDPE/PET Blends Presenting Different Phase Morphologies. *Polym. Eng. Sci.* **2005**, *45*, 354–363. [CrossRef]
13. Nomura, K.; Peng, X.; Kim, H.; Jin, K.; Kim, H.J.; Bratton, A.F.; Bond, C.R.; Broman, A.E.; Miller, K.M.; Ellison, C.J. Multiblock Copolymers for Recycling Polyethylene–Poly(Ethylene Terephthalate) Mixed Waste. *ACS Appl. Mater. Interfaces* **2020**, *12*, 9726–9735. [CrossRef] [PubMed]
14. Tang, X.; Liu, C.; Keum, J.; Chen, J.; Dial, B.E.; Wang, Y.; Tsai, W.-Y.; Bras, W.; Saito, T.; Bowland, C.C.; et al. Upcycling of Semicrystalline Polymers by Compatibilization: Mechanism and Location of Compatibilizers. *RSC Adv.* **2022**, *12*, 10886–10894. [CrossRef]
15. Yousfi, M.; Soulestin, J.; Vergnes, B.; Lacrampe, M.F.; Krawczak, P. Morphology and Mechanical Properties of PET/PE Blends Compatibilized by Nanoclays: Effect of Thermal Stability of Nanofiller Organic Modifier. *J. Appl. Polym. Sci.* **2013**, *128*, 2766–2778. [CrossRef]
16. Papadopoulou, C.P.; Kalfoglou, N.K. Comparison of Compatibilizer Effectiveness for PET/PP Blends: Their Mechanical, Thermal and Morphology Characterization. *Polymer* **2000**, *41*, 2543–2555. [CrossRef]
17. Kalfoglou, N.K.; Skafidas, D.S.; Sotiropoulou, D.D. Compatibilization of Blends of Poly(Ethylene Terephthalate) and Linear Low Density Polyethylene with the Ionomer of Poly(Ethylene-Co-Methacrylic Acid). *Polymer* **1994**, *35*, 3624–3630. [CrossRef]
18. Friedrich, K.; Evstatiev, M.; Fakirov, S.; Evstatiev, O.; Ishii, M.; Harrass, M. Microfibrillar Reinforced Composites from PET/PP Blends: Processing, Morphology and Mechanical Properties. *Compos. Sci. Technol.* **2005**, *65*, 107–116. [CrossRef]
19. Akshaya, E.M.; Palaniappan, R.; Sowmya, C.F.; Rasana, N.; Jayanarayanan, K. Properties of Blends from Polypropylene and Recycled Polyethylene Terephthalate Using a Compatibilizer. *Mater. Proc.* **2020**, *24*, 359–368. [CrossRef]
20. Galgani, F.; Hanke, G.; Maes, T. Global Distribution, Composition and Abundance of Marine Litter. In *Marine Anthropogenic Litter*; Bergmann, M., Gutow, L., Klages, M., Eds.; Springer International Publishing: Cham, Switzerland, 2015; pp. 29–56, ISBN 978-3-319-16510-3.
21. Hetemi, D.; Pinson, J. Functionalization of Polymers by Hydrolysis, Aminolysis, Reduction, Oxidation, and Some Related Reactions. In *Surface Modification of Polymers*; Wiley-VCH: Weinheim, Germany, 2019; pp. 211–240, ISBN 978-3-527-81924-9.
22. Lepoittevin, B.; Costa, L.; Pardoue, S.; Dragoé, D.; Mazerat, S.; Roger, P. Hydrophilic PET Surfaces by Aminolysis and Glycopolymer Brushes Chemistry. *J. Polym. Sci. Part Polym. Chem.* **2016**, *54*, 2689–2697. [CrossRef]
23. Xu, T.; Li, Z.; Ju, X.; Tang, H.; Xiang, W. Chemical Degradation of Waste PET and Its Application in Wood Reinforcement and Modification. *ACS Omega* **2023**, *8*, 30550–30562. [CrossRef] [PubMed]
24. Kárpáti, L.; Ganyecz, Á.; Nagy, T.; Hamar, G.; Banka, E.; Kállay, M.; Vargha, V. Synthesis and Characterization of Isophorondiamine-Based Oligoamides: Catalytic Effect of Amides during the Curing of Epoxy Resins. *Polym. Bull.* **2020**, *77*, 4655–4678. [CrossRef]

25. Hoang, C.N.; Dang, Y.H. Aminolysis of Poly(Ethylene Terephthalate) Waste with Ethylenediamine and Characterization of α,ω-Diamine Products. *Polym. Degrad. Stab.* **2013**, *98*, 697–708. [CrossRef]
26. Ghosal, K.; Nayak, C. Recent Advances in Chemical Recycling of Polyethylene Terephthalate Waste into Value Added Products for Sustainable Coating Solutions—Hope vs. Hype. *Mater. Adv.* **2022**, *3*, 1974–1992. [CrossRef]
27. Heidari, S.; Tahvildari, K. Preparation and Characterization of Diols and Polyols Based on Aminolysis of Poly (Ethylene Terephthalate) Wastes with Alkanolamines. *J. Appl. Chem. Res.* **2013**, *7*, 33–42.
28. Suhaimi, N.A.S.; Muhamad, F.; Abd Razak, N.A.; Zeimaran, E. Recycling of Polyethylene Terephthalate Wastes: A Review of Technologies, Routes, and Applications. *Polym. Eng. Sci.* **2022**, *62*, 2355–2375. [CrossRef]
29. Spychaj, T.; Fabrycy, E.; Spychaj, S.; Kacperski, M. Aminolysis and Aminoglycolysis of Waste Poly(Ethylene Terephthalate). *J. Mater. Cycles Waste Manag.* **2001**, *3*, 24–31. [CrossRef]
30. Aminolysis of Polyesters for Cracking and Structure Clarifying: A Review—Rabiei—2022—Polymers for Advanced Technologies—Wiley Online Library. Available online: https://onlinelibrary.wiley.com/doi/10.1002/pat.5837 (accessed on 12 April 2023).
31. Todd, A.D.; McEneany, R.J.; Topolkaraev, V.A.; Macosko, C.W.; Hillmyer, M.A. Reactive Compatibilization of Poly(Ethylene Terephthalate) and High-Density Polyethylene Using Amino-Telechelic Polyethylene. *Macromolecules* **2016**, *49*, 8988–8994. [CrossRef]
32. Kamatani, H.; Konagaya, S.; Nakamura, Y. Effect of Phosphoric Acid on the Polycondensation of Bis(2-Hydroxyethyl) Terephthalate Catalyzed by Sb(III) Compounds. *Polym. J.* **1980**, *12*, 125–130. [CrossRef]
33. *ASTM D3418*; A Standard Test Method for Transition Temperatures and Enthalpies of Fusion and Crystallization of Polymers by Differential Scanning Calorimetry. ASTM: Philadelphia, PA, USA, 2021.
34. Mehta, A.; Gaur, U.; Wunderlich, B. Equilibrium Melting Parameters of Poly(Ethylene Terephthalate). *J. Polym. Sci. Polym. Phys. Ed.* **1978**, *16*, 289–296. [CrossRef]
35. Gao, M.; Jiao, Q.; Cui, W.; Feng, C.; Zhao, Y.; Xiang, A.; Mu, X.; Ma, L. Preparation of PET/LDH Composite Materials and Their Mechanical Properties and Permeability for $O_2$. *Polym. Eng. Sci.* **2019**, *59*, E366–E371. [CrossRef]
36. Pretsch, E.; Bühlmann, P.; Badertscher, M. (Eds.) IR Spectroscopy. In *Structure Determination of Organic Compounds: Tables of Spectral Data*; Springer: Berlin/Heidelberg, Germany, 2020; pp. 307–373, ISBN 978-3-662-62439-5.
37. Badía, J.D.; Vilaplana, F.; Karlsson, S.; Ribes-Greus, A. Thermal Analysis as a Quality Tool for Assessing the Influence of Thermo-Mechanical Degradation on Recycled Poly(Ethylene Terephthalate). *Polym. Test.* **2009**, *28*, 169–175. [CrossRef]
38. Litmanovich, A.D.; Platé, N.A.; Kudryavtsev, Y.V. Reactions in Polymer Blends: Interchain Effects and Theoretical Problems. *Prog. Polym. Sci.* **2002**, *27*, 915–970. [CrossRef]
39. Kasapoglu, F.; Cianga, I.; Yagci, Y.; Takeichi, T. Photoinitiated Cationic Polymerization of Monofunctional Benzoxazine. *J. Polym. Sci. Part Polym. Chem.* **2003**, *41*, 3320–3328. [CrossRef]


**Disclaimer/Publisher's Note:** The statements, opinions and data contained in all publications are solely those of the individual author(s) and contributor(s) and not of MDPI and/or the editor(s). MDPI and/or the editor(s) disclaim responsibility for any injury to people or property resulting from any ideas, methods, instructions or products referred to in the content.